

1 **Radial Glia cell infection by *Toxoplasma gondii***
2 **disrupts brain microvascular endothelial cell integrity**

3 Daniel Adesse^{1*}, Anne Caroline Marcos¹, Michele Siqueira², Cynthia M. Cascabulho³,
4 Mariana C. Waghbi⁴, Helene S. Barbosa¹, Joice Stipursky^{2*}.

5 **Affiliation:** 1) Laboratório de Biologia Estrutural, Instituto Oswaldo Cruz, Fiocruz; 2) Laboratório de
6 Neurobiologia Celular, ICB, UFRJ; 3) Laboratório de Inovação em Terapias, Ensino e Bioprodutos, Instituto
7 Oswaldo Cruz, Fiocruz; 4) Laboratório de Genômica Funcional e Bioinformática, Instituto Oswaldo Cruz,
8 Fiocruz.

9
10 ***Corresponding authors:** joice@icb.ufrj.br; daniel.adesse@gmail.com

11 **Key words:** congenital toxoplasmosis, *Toxoplasma gondii*, TORCH, radial
12 glia, endothelial cells, brain development, neurogenesis, blood brain barrier.

13 **Running Title:** *Toxoplasma gondii* impairs neurovascular interactions

14 **8705 Words manuscript**

15 **27 Pages**

16 **3 Figures**

17 **2 Supplementary figures**
18
19
20
21
22
23
24
25
26
27
28

29 **ABSTRACT (228)**

30 Congenital toxoplasmosis is a parasitic disease that occurs due vertical transmission
31 of the protozoan *Toxoplasma gondii* (*T. gondii*) during pregnancy. The parasite crosses the
32 placental barrier and reaches the developing brain, infecting progenitor, glial, neuronal and
33 vascular cell types. Although the role of Radial glia (RG) neural stem cells in the
34 development of the brain vasculature has been recently investigated, the impact of *T. gondii*
35 infection in these events is not yet understood. Herein, we studied the role of *T. gondii*
36 infection on RG cell function and its interaction with endothelial cells. By infecting isolated
37 RG cells with *T. gondii* tachyzoites, we observed reduced cell proliferation and
38 neurogenesis without affecting gliogenesis levels. Conditioned medium (CM) from RG
39 control cultures increased ZO-1 and β -catenin protein levels and organization on
40 endothelial bEnd.3 cells membranes, which was completely impaired by CM from infected
41 RG, resulting in decreased transendothelial electrical resistance (TEER). Cytokine Bead
42 Array and ELISA assays revealed the presence of increased levels of the pro-inflammatory
43 cytokine IL-6 and reduced levels of anti-inflammatory cytokine TGF- β 1 in CM from *T.*
44 *gondii*-infected RG cells. Treatment with recombinant TGF- β 1 concomitantly with CM from
45 infected RG cultures led to restoration of ZO-1 staining in bEnd.3 cells. Our results suggest
46 that infection of RG cells by *T. gondii* modulate cytokine secretion, which might contribute to
47 endothelial loss of barrier properties, thus leading to impairment of neurovascular
48 interaction establishment.

49

50

51 **1) INTRODUCTION (904)**

52 Toxoplasmosis is a parasitic disease that affects all warm-blooded animals, including
53 humans. The disease is caused by a protozoan parasite, *T. gondii* and has a high global
54 seroprevalence, estimated in approximately 1/3 of the world's population (Dubey, 2010).
55 Transmission occurs by ingestion of uncooked meat from infected animals, that contains
56 tissue cysts, or by ingestion or inhalation of sporulated oocysts, shed with feces of infected
57 felids. The cysts are digested by proteolytic enzymes present in the stomach and small
58 intestine, which then release infective parasites that rapidly invade epithelial cells of the
59 small intestine and differentiate into fast-replicating tachyzoite forms. After intense
60 intracellular proliferation, parasites promote host cell lysis and can disseminate throughout
61 the entire organism (reviewed in Hill and Dubey, 2016). During the acute phase, patients
62 may present lymphadenopathy, which may be associated with fever, fatigue, muscle pain,
63 sore throat and headaches (Montoya and Liesenfeld, 2004).

64 *T. gondii* can also be vertically transmitted during gestation, leading to Congenital
65 Toxoplasmosis (CT), established by the capacity of the parasite to cross the placental
66 barrier and reach the developing brain tissue, where both tachyzoites and tissue cysts can
67 be found in the developing brain parenchyma (Ferguson et al., 2013). CT is part of the
68 TORCH complex of infectious diseases (**T**oxoplasma, **R**ubella, **C**ytomegalovirus, **H**erpes
69 simplex 2. **O** stands for Others, and includes chlamydia, HIV, Coxsackievirus, Syphilis,
70 Hepatitis B, chicken pox and Zika virus) that can be transmitted from the mother to the fetus
71 (Neu et al., 2015; Mehrjadi, 2017). Infection with some of these pathogens can potentially
72 lead to congenital defects including, but not limited to, microcephaly, growth and mental
73 retardation, heart disease and hearing loss (Neu et al., 2015; Klase et al., 2016). Although
74 transmission during the third trimester has been implicated in reduced impact on the fetus,
75 infection during the first trimester is extremely disruptive, with severe neurological
76 manifestations including microcephaly, cognitive/intellectual disabilities, deafness and
77 blindness (Wallon et al., 1999).

78 Deleterious effects of infection of mouse neural progenitor cells by a highly infective
79 *T. gondii* strain was linked to apoptosis induction by endoplasmic reticulum stress signaling
80 pathway activation (Wang et al., 2014). In addition, reduced neuron and astrocyte
81 generation from the neural C17.2 stem cell line by disruption of the Wnt/ β -catenin signaling
82 pathway have also been suggested as an underlying mechanism of *T. gondii*-induced
83 neural pathological damage during brain development (Gan et al., 2016; Zhang et al.,
84 2017).

85 RG cells are the major multipotent neural stem cell population present during the
86 embryonic cerebral cortex development period and originate most of the neuronal and glial
87 cell types found in neural tissue, by activation of multiple signaling pathways (Gotz and
88 Barde, 2005; Kriegstein and Alvarez-Buylla, 2009; Stipursky et al., 2012; Stipursky et al.,
89 2014). Besides its well-known role as neural stem cells, RG have recently been
90 demonstrated to directly control vascular development and blood brain barrier (BBB)
91 formation in the embryonic cerebral cortex (Ma et al., 2013; Errede et al., 2014; Hirota et
92 al., 2015; Siqueira et al., 2017).

93 We have previously demonstrated that the gliogenic and neurogenic potential of RG
94 cells during cerebral cortex development is controlled by TGF- β 1 signaling pathway
95 activation, both *in vitro* and *in vivo* (Stipursky et al., 2012; Stipursky et al., 2014).
96 Neuroepithelial and RG neural progenitors interact with immature endothelial cells, derived
97 from the perineural vascular plexus (PNVP) that surrounds the neural tissue early during
98 the embryonic period. Such an interaction is essential to promote invasion of endothelial
99 cells and vascularization of the developing CNS. Endothelial cells from the PNVP invade
100 forebrain tissue as early as E9.5 in mice and migrate towards the ventricular surface,
101 guided by VEGF gradients secreted by neural progenitor cells (Bautch and James, 2009;
102 Anderson et al., 2011; Liebner et al., 2011; Takahashi et al., 2015). Recently, we
103 demonstrated that RG cells coordinate the formation of the vascular tree of the brain, by
104 controlling angiogenesis in the developing cortex. Specifically, RG cells secrete a vast

105 repertoire of pro-angiogenic factors, including TGF- β 1 and VEGF-A, that induce endothelial
106 proangiogenic genes expression and regulate migration and blood vessel branching in the
107 embryonic cerebral cortex (Siqueira et al., 2017).

108 Blood vessel development and neural cell generation in the CNS are essential steps
109 for the establishment of the BBB. The BBB is a multicellular structure formed by capillary
110 endothelial cells, astrocytic endfeet, pericytes and neighboring microglia and neurons, that
111 control the transport of nutrients, oxygen and other substances, and prevent the free
112 passage of toxic agents and pathogens (Kim et al., 2006; Anderson et al., 2011). In the
113 adult brain, *T. gondii* can infect endothelial cells (Konradt et al., 2016) and, by modulation of
114 adhesion proteins, contribute to decreased adhesion between adjacent endothelial,
115 allowing for transmigration of inflammatory cells into the brain parenchyma (Lachenmaier et
116 al., 2011).

117 Although RG physiology greatly determines the correct formation of the cerebral
118 cortex, including its vascularization (Ma et al., 2013; Errede et al., 2014; Hirota et al., 2015;
119 Siqueira et al., 2017), the understanding of the impact of *T. gondii* infection on RG-
120 endothelial interactions in the embryonic CNS has never been addressed.

121 Here, we investigated the role of *T. gondii* infection on RG physiology and its potential
122 to control endothelial barrier properties establishment. We demonstrated that infection
123 reduce the neurogenesis potential and altered the RG secretome. Such altered alterations
124 lead to important dysfunctions in microvascular brain endothelial cells, presenting reduced
125 tight junction stability and barrier properties when incubated with a conditioned medium
126 obtained from infected RGs.

127

128 **2) MATERIAL AND METHODS (1229)**

129 **2.1) Compliance with Ethical Standards:** All animal protocols were approved by the
130 Federal University of Rio de Janeiro Animal Research Committee (CEUA 041/14). Animals

131 were housed in a temperature-controlled room with a 12/12 h light/dark cycle and allowed
132 food and water *ad libitum*.

133 **2.2) *Toxoplasma gondii* infection:** Parasites from the ME49 strain were obtained
134 from the brains of C57/bl6 mice infected 45 days before isolation. Cysts were ruptured with
135 an acid pepsin solution and free parasites were added to monolayers of Vero cells
136 (ATCC® CCL-81™). After two weeks of culture re-infections, tachyzoites released from the
137 supernatant were collected and centrifuged. Cell cultures were infected with the tachyzoites
138 at a multiplicity of infection (MOI) of 3 parasites:host cell (Luder et al., 1999) for 2 hours in
139 300 µL of DMEM-/F12/2% B27/ Penicilin-streptocycin (Thermo) (RG cultures). Cells were
140 washed in Ringer's solution, fresh culture media was added, and cultures were kept for
141 additional 22 hours, when conditioned medium was collected and cells fixed for
142 immunostaining. Mock-infected cultures (treated with fresh culture medium) were used as
143 controls.

144 **2.3) Radial glia (RG) cultivation:** RG isolation from E14 gestational day-old Swiss
145 mouse embryos was carried out as previously described by Stipursky et al. (2014). Briefly,
146 gestational day14 Swiss mice embryos were collected and dissected for cerebral cortex
147 separation. After dissection, tissues were dissociated in DMEM/F12 Glutamax high glucose
148 (Thermo) medium and after cell counting, $3 \cdot 10^5$ cells were plated in 25 cm² culture flasks in
149 neurosphere "growing media" DMEM/F12 Glutamax high glucose (Thermo) containing
150 0.1% penicillin/streptomycin, 2% B27 (Thermo), 20ng/mL EGF (epidermal growth factor,
151 Thermo) and 20 ng/mL FGFb (basic fibroblast growth factor, R&D Systems), for 6 days, *in*
152 *vitro*. 2/3 of the media was changed every 2 days. After this period, neurospheres were
153 enzymatically dissociated in 0.05%Trypsin/EDTA (Thermo). After cells isolation, $2 \cdot 10^5$ cells
154 were plated on glass coverslips previously coated with 5 µg/mL laminin (Thermo) and
155 incubated in DMEM/F12 Glutamax (high glucose) without serum and supplemented with
156 2% B27, 20 ng/mL FGFb and EGF (Thermo). Twenty-four hours after plating, cells were
157 infected with the tachyzoite forms of the *T. gondii*, ME49 strain as described above. After
158 infection, cells were gently washed to remove extracellular parasites and 300 µL of fresh

159 DMEM/F12/ medium were added, followed by 22 hours of incubation. Next, non-infected
160 and infected RG cells were fixed with paraformaldehyde 4% solution in PBS (Sigma-
161 Aldrich) for immunocytochemistry assays. Supernatants were collected, centrifuged for 10
162 min at 10,000 rpm (4 °C) to eliminate cell debris and extracellular parasites and frozen at -
163 80 °C to be further used as a Conditioned Medium (CM) or for cytokine measurements.

164 **2.4) Enzyme-Linked Immunosorbent Assay (ELISA):** TGF- β 1 levels present in the
165 conditioned medium derived from non-infected (RG-CM) and infected (Inf-RG-CM) RG
166 cells, were measured by the Mouse TGF- β 1 ELISA DuoSet Kit (R&D Systems) following
167 the manufacturer's instructions.

168 **2.5) Cytometric Bead Array (CBA):** Cytokine levels were evaluated by flow
169 cytometry in culture RG-CM and Inf-RG-CM supernatants. IL-10, IL-17, TNF, IFN- γ , IL-6, IL-
170 4 and IL-2 were detected using a Cytometric Bead Array (CBA) Th1/Th2/TH17 kit (BD),
171 according to the manufacturer's instructions. Samples were acquired using a FACScalibur
172 flow cytometer (BD), and the data analysis was performed using the CBA analysis FCAP
173 software (BD).

174 **2.6) bEnd.3 cell line cultivation:** A total of 6.10^4 murine brain microvascular
175 endothelial cells (bEnd.3, ATCC[®] CRL-2299[™]) were plated on glass coverslips previously
176 coated with 0.01% porcine gelatin solution (Sigma-Aldrich) in bEnd.3 medium [DMEM/F12
177 Glutamax high glucose (4500 mg/L) with 10% heat-inactivated Fetal Bovine Serum
178 (Cultilab) and 1% penicillin/streptomycin solution (Thermo)] for 14 days, with the medium
179 changed every 2 days. After reaching confluence, cultures were treated with RG-CM, Inf-
180 RG-CM, Inf-RG-CM+TGF- β 1 (10ng/ML, R&D Systems) or TGF- β 1 (10ng/mL) for 24 hours.
181 Cultures were fixed with PFA 4% for immunocytochemistry assays. Cells were used
182 between passages 25 to 30.

183 **2.7) Immunocytochemistry:** Immunostaining was performed as previously described
184 by Siqueira et al. (2017). Briefly, fixed cultures were permeabilized for 5 min with 0.05%
185 Triton x-100 solution in PBS and non-specific binding blocked by incubation with blocking
186 solution containing 5% Bovine Serum Albumin (BSA - Sigma-Aldrich)/2.5% Normal Goat

187 Serum (NGS)/PBS for 1 hour. Cells were incubated with primary antibodies, diluted in
188 blocking solution and maintained overnight at 4°C. For RG cultures, immunostaining
189 primary antibodies were: mouse anti-Nestin (marker of neural progenitor cells, Millipore,
190 1:200); rabbit anti-BLBP (marker of radial glia cells, Chemicon, 1:500), rabbit anti-Ki67
191 (nuclear marker of mitotic cells, Abcam, 1:100), rabbit anti-GFAP (intermediary filament
192 protein specific to glial cells, Dako Cytomation, 1:500) and mouse anti- β -III-tubulin (specific
193 isoform found in immature neurons, Promega, 1:1000), and mouse anti-cleaved Caspase 3
194 (apoptosis cell marker, Abcam, 1:100). For endothelial culture immunostaining, primary
195 antibodies were: mouse anti-ZO-1 (Invitrogen, 1:300), rabbit anti- β -catenin (Sigma-Aldrich,
196 1:200). Subsequently, cells were extensively washed in PBS and incubated with secondary
197 antibodies, conjugated to AlexaFluor 488 or AlexaFluor 546 (Thermo), for 2 h at room
198 temperature. Nuclei were DAPI-labeled (4', 6-Diamidino-2-phenylindole; Sigma-Aldrich).
199 Glass coverslips were mounted in glass slides with Faramount mounting media (Dako
200 Cytomation) and visualized under a fluorescence optical microscope Nikon TE3000 or a
201 Leica SPE confocal microscope. Fifteen random images under a 40x objective were
202 acquired from each glass coverslip from at least 3 independent experiments done in
203 triplicate.

204 **2.8) Trans-Endothelial Electrical Resistance (TEER):** bEnd.3 cells were plated
205 onto 0.01% gelatin-coated Transwell inserts (Falcon) with 3 μ m pores at a density of 10^5
206 cells per insert. Cultures were maintained in bEnd.3 medium at 37°C in 5% CO₂
207 atmosphere and resistance was measured daily using a Millicell-Electrical Resistance
208 System (Millipore, Bedford, MA) with an adjustable electrode ("chopstick electrode",
209 MERSSTX03), as described by Srinivasan et al., 2015. Cells reached confluence after
210 approximately 14 days (minimum of 60 Ω x cm²), with the medium changed every 2 days.
211 One electrode is inserted into the upper trans-well insert compartment and the other
212 electrode to the lower compartment. Care is taken to ensure that all compartments have the
213 same volume of medium across biological and technical replicas (300 ml in the upper
214 compartment and 600 ml in the lower). A square wave current of 12.5 Hz is applied to the

215 electrodes and the resulting current is measured. To calculate TEER, the background
216 resistance reading from an empty insert was subtracted from the resistance reading for
217 each condition and the result was multiplied by 0.33, relative to the insert area, and results
218 were expressed as $\Omega \times \text{cm}^2$. One insert per experiment was maintained in bEnd.3 medium
219 (10% FBS), while experimental data was obtained from cultures incubated with DMEM/F12
220 high glucose with antibiotics solution and no FBS. Cells were used for experiments when
221 TEER reached a minimum of $60 \Omega \times \text{cm}^2$. TEER was obtained before experimental
222 procedures ($t=0$) and 24 h after treatments with CMs or infection ($t=24$). The variation index
223 for each experimental condition was calculated as $\text{TEER}_{t=24}/\text{TEER}_{t=0}$.

224 **2.9) Quantification and statistical analyses:** Quantification analyses of cell
225 populations (RG, neurons and astrocytes) were carried out manually using the Photoshop
226 CS6 software. The percentage of each stained cell population, in each microscopic field,
227 was calculated in relation to total DAPI stained cells numbers in the same field. bEnd.3
228 labeling intensity analysis was carried out using the ImageJ software and the TiJOR
229 analysis was performed using the TiJOR macro for ImageJ, which in an index of localization
230 of tight junction proteins in membrane-membrane contact region of adjacent cells as
231 described by Terryn et al. (2013). The GraphPad Prism 6.0 software was used for the
232 statistical analyses, obtained at <http://www.graphpad.com/scientific-software/prism>.
233 Statistical significance from at least 3 independent experiments was determined by
234 unpaired t-test and ANOVA for biological effects with an assumed normal distribution. P
235 value <0.05 was considered statistically significant.

236

237

238 **3) RESULTS (767)**

239

240 **3.1) *T. gondii* infection alters Radial Glia cell numbers and neurogenesis.**

241 In order to understand the effects of *T. gondii* infection on the RG differentiation
242 potential, isolated RG cells from E14 cerebral cortex were infected with the tachyzoite forms
243 of the parasite. We used the cells 24 hours after neurosphere dissociation and plating. At
244 this time, Radial glia cultures are virtually pure with 96% of cells positive for blbp and 95.7%
245 positive for nestin (92% were blbp/nestin double positive, Stipursky J., personal
246 communications). After 24 hours of infection with *T. gondii*, mock-infected (control) cells
247 displayed typical radial bipolar morphology and expression of typical RG neural stem cells
248 markers BLBP and Nestin, *in vitro* (**Figure 1A**). Parasites were detected in the cytoplasm of
249 Nestin-positive cells (**Supplementary Figure 1C-D**). Infected cultures presented a 40%
250 decrease in the number of BLBP/Nestin double-labeled cells (**Figure 1 A-C**). This event
251 was accompanied by a 25 % decrease in proliferative RG cells double labeled for Ki67 and
252 Nestin markers (**Figure 1 D-E**). In parallel, *T. gondii* infection also significantly decreased
253 the numbers of early neurons (as detected by β -III-tubulin labeling) by 36% (**Figure 1 G-I**).
254 However, no effect on the number of astrocytic (GFAP-positive) cells was detected in
255 infected cultures compared to the controls (**Figure 1 J-L**). The average of total cells number
256 of β -TubulinIII and Nestin positive cells double labeled for the apoptotic marker cleaved-
257 Caspase 3 was not affected by infection (**Supplementary Figure 2A**). Overall, *T. gondii*-
258 infected cultures presented a shift in the percentage of cell composition when compared to
259 uninfected controls, with Nestin/BLBP and β -III-tubulin positive cells being directly affected,
260 although other unidentified cell types also tended to present percentage alterations,
261 increasing from 17% in controls to 40% in infected cultures (**Figure 1M**).

262

263 **3.2) *T. gondii* infection affects RG potential to control endothelial barrier property.**

264 To investigate the potential of RG cells to control endothelial cells function and the
265 role of *T. gondii* infection in this context, we cultivated b.End3 endothelial cells until

266 confluence. Through immunocytochemistry analyses, we identified ZO-1 adapter tight
267 junction protein mainly distributed along cell-cell contacts in the control condition (**Figure**
268 **2A**). Treatment of endothelial cells with conditioned medium derived from uninfected RG
269 cells (RG-CM) for 24 h significantly increased the ZO-1 labeling intensity levels by 36%
270 (**Figure 2B, D**). This was concomitant with an increase in organization levels of the tight
271 junctions (TiJOR) by 90% (**Figure 2 E**). However, treatment of endothelial cells with
272 conditioned medium derived from infected RG cells (Inf-RG-CM) completely abrogated RG
273 potential to induce ZO-1 labeling intensity, by 40%, when compared to control cultures,
274 although the TiJOR index did not differ from the controls (**Figure 2 C, D**). In summary, Inf-
275 RG-CM-treated presented deleterious effects on tight junction protein levels and
276 organization.

277 Additionally, a functional trans-endothelial electrical resistance (TEER) assay was
278 performed to investigate whether the structural tight junction modifications observed herein
279 were accompanied by alterations in endothelial monolayer barrier properties. Cultivation of
280 endothelial cells with RG-CM for 24 h increased TEER barrier properties by 22%. However,
281 addition of Inf-RG-CM completely impaired RG-induced increases in barrier properties,
282 although no significant alterations were observed in cell morphology. Treatment with Inf-
283 RG-CM decreased TEER barrier properties by 27% when compared to the controls (**Figure**
284 **2 F**).

285 The role of RG infection on the distribution of the pro-angiogenic signaling protein β -
286 catenin in endothelial cells was also investigated. The deleterious effect of Inf-RG-MC seen
287 in TiJOR and TEER was also true for β -catenin protein distribution on bEnd.3 cells
288 monolayers. In the control condition, β -catenin colocalized with ZO-1 along cell-cell
289 contacts (**Figure 2 G, J, M**). The RG-CM treatment significantly increased β -catenin
290 immunolocalization at junctional regions, which was impaired by Inf-RG-CM treatment
291 (**Figure 2 H, K, N and I, L, O**).

292

293 **3.3) *T. gondii*-infected RG cultures present altered cytokine secretion that**
294 **affects endothelial cell barrier properties.**

295 To gain insight into the possible alterations induced by *T. gondii* on the RG secretory
296 protein repertoire, a CBA analysis was carried out to measure the inflammation related
297 factors IL-2, IL-4, IL-6, IL-10, IL-17, IFN- γ and TNF- α , followed by an ELISA analysis for
298 the neuroprotector TGF- β 1, to measure the levels of these cytokines in the RG-CM and
299 Inf-RG-CM. No detectable levels of IL-2, IL-4, IL-10, IL-17, IFN- γ and TNF- α , in the
300 conditioned mediums were observed. CM from infected RG cultures showed IL-6 in
301 increased concentrations (7.4 pg/ml) when compared to CM from control RG-CM (0.3
302 pg/ml, $p < 0.01$, unpaired *t* test). TGF- β 1 levels were 40% decreased in Inf-RG-CM when
303 compared to uninfected cultures (18 versus 29 pg/ml, $p < 0.05$, Unpaired Student's T test)
304 **(Figure 3A).**

305 Since TGF- β 1 has a crucial role on brain microvasculature, we treated bEnd.3 cells
306 with Inf-RG-CM together with recombinant TGF- β 1 (10ng/mL) for 24 hours and performed
307 immunocytochemistry for ZO-1. Addition of TGF- β 1 to Inf-RG-CM completely rescued the
308 ZO-1 labeling intensity to levels comparable to RG-CM condition, similarly to addition of
309 TGF- β 1 alone **(Figure 3 B).**

310

311

312 **4. DISCUSSION (2200)**

313

314 **4.1) RG differentiation potential is impaired by *T. gondii* infection**

315 RG cells have been extensively investigated concerning several features, including
316 neuronal migration support and multipotent neural stem cell potential in generating neurons,
317 astrocytes, oligodendrocytes and other progenitor subtypes in the cerebral cortex (Rakic,
318 1999; Noctor et al., 2001; Morest and Silver, 2003; Barnabe-Heider et al., 2005; Stipursky
319 and Gomes, 2007; Kessarlis et al., 2008; Kriegstein and Alvarez-Buylla, 2009; Ortega and
320 Alcantara, 2010; Stipursky et al., 2012; Stipursky et al., 2014). Evidence suggest that neural
321 progenitors are directly affected by the TORCH complex of perinatal infectious diseases
322 that, ultimately, lead to malformations in the cerebral cortex, such as microcephaly, mostly
323 by disrupting neural cells generation (Neu et al., 2015). Regarding infection with *T. gondii*,
324 recent findings point to increased apoptosis and reduced cell differentiation in the C17.2
325 neural stem cell line (Gan et al., 2016; Wang et al., 2014; Zhang et al., 2017). However,
326 further characterization and evaluation of the effects of *T. gondii* infection on primary RG
327 cells isolated from embryonic cerebral cortex have not yet been addressed. The present
328 study indicates that *T. gondii* significantly decreases the number of Nestin/BLBP positive
329 RG cells, possibly by decreasing their proliferation. Accordingly, previous data describe that
330 altered neural stem cell proliferation, differentiation and apoptosis can be triggered by viral
331 infection (Gan, 2016; Souza et al., 2016). In our model, RG cells accounted for 51% of the
332 total cell population in the control condition after a total period of 48 h of cultivation. Since
333 the total number of cells and the small percentage of apoptotic RG cells were not affected
334 by *T. gondii* infection, it is possible that global cytotoxic infection effects were not the
335 mechanism leading to reduced numbers of, specifically, Nestin/BLBP positive RG cells.
336 Although RG cells have been described by our group and others to differentiate into
337 astrocytes at later stages of cortical development (Rakic, 1971; de Azevedo et al., 2005;
338 Stipursky and Gomes, 2007; Stipursky et al., 2012; Stipursky et al., 2014), no alterations in
339 astrocyte differentiation by *T. gondii* infection were observed. Secreted levels of IL-6 and

340 TGF- β 1, two cytokines known to positively mediate astrocyte differentiation from neural
341 progenitor cells (Taga and Fukuda, 2005; Nakamura et al., 2005, Stipursky and Gomes,
342 2007; Stipursky et al., 2012; Stipursky et al., 2014), were altered in Inf-RG-CM. However, it
343 is possible that, in this context, altered cytokine levels might not control autocrine regulation
344 of astrocytogenesis, or that other molecular mechanisms known to modulate gliogenesis
345 are not altered in this context. On the other hand, a reduction in β -III-tubulin positive cell
346 numbers was detected, without affecting apoptotic neuronal population, suggesting
347 inhibition of neurogenesis. This finding is corroborated by the recent demonstration that *T.*
348 *gondii* infection impairs neuron generation from C17.2 neural stem cell line *in vitro* (Gan et
349 al., 2016; Zhang et al., 2017). However, it is possible that, in addition to *T. gondii* induced
350 alterations of well-known molecular mechanisms that control neurogenesis during cortical
351 development, such as Wnt/ β cat signaling (Gan et al., 2016; Zhang et al., 2017) and
352 neuronal differentiation transcription factors, such as Fabp7/BLBP, Sox2, Tacc3 Eya1,
353 Sox2, and Tnfrsf12a genes (Xiao et al., 2012), altered levels of IL-6, TGF- β 1 and other, still
354 unidentified cytokines, might exert an autocrine effect on the neurogenic potential of RG
355 cells. Although *T. gondii* infection decreased the number of Nestin/BLBP and β -III-tubulin
356 positive cells and did not alter GFAP cells numbers, overall cell composition percentages
357 induced an increase in an unidentified cell population, suggesting that RG differentiation
358 might favor the appearance of other cell types. Thus, since the literature lacks a more
359 detailed investigation regarding the impact of congenital transmission of *T. gondii* in
360 cerebral cortex embryonic development *in vivo*, it is essential to address how neurogenesis
361 and/or gliogenesis are affected during CT in the developing brain.

362

363 **4.2) Impacts of *T. gondii* infection on RG potential to control endothelial** 364 **barrier properties.**

365 Vascular development by angiogenesis, in addition to blood vessel stability and
366 function, result from a fine-tuned control of pro- and anti-angiogenic molecules
367 produced by endothelial and neighboring cells, as well as environmental cues

368 (Carmeliet and Jain, 2000). In the last few years, RG have been pointed out as an
369 essential cellular and molecular scaffold for blood vessel formation and vascular
370 stability acquisition during cerebral cortex development (Ma et al., 2013; Errede et al.,
371 2014; Hirota et al., 2015; Siqueira et al., 2017). Herein, we demonstrate that RG-CM
372 treatment of endothelial cells greatly increases tight junction ZO-1 protein levels and
373 organization, suggesting that RG-secreted factors promote microvascular barrier
374 formation. Vascular stability and barrier properties are essential features that allow
375 the controlled transport of nutrients and other substances across the BBB (Abbott,
376 2005; Ben-Zvi et al., 2014). Several molecular mechanisms were shown to promote
377 the expression of tight junction proteins Claudin-5, Occludin and ZO-1 in endothelial
378 cells, thus leading to the formation of the BBB, including activation of the TGF- β 1
379 signaling pathway, PDGFR/PDGR-B interaction and Wnt/ β catenin (Alvarez et al.,
380 2011; Baeten and Akassoglou, 2011; Zhao et al., 2014; Zhao et al., 2015). In this
381 context, *T. gondii* infection may indirectly deregulate signaling pathways critical in
382 controlling vessel stability by (i) affecting RG potential concerning mediation of BBB
383 formation or (ii) disrupting tight junction proteins expression and organization directly
384 in endothelial cells. Increased BBB disruption and permeability have been recently
385 correlated t elevated levels of the pro-inflammatory cytokine IL-6 in the cerebrospinal
386 fluid of human adult individuals affected by neuromyelitis optica and neuropsychiatric
387 systemic lupus erythematosus, and in a rat model of psychosocial stress induction
388 (Uchida et al., 2017; Asano et al., 2017; Schiavone et al., 2017).

389 Pro-inflammatory cytokines, such as IL-6, have been previously reported to promote
390 BBB dysfunction in several neurodegenerative disease contexts, such as Alzheimer's,
391 Parkinson's and Multiple sclerosis, as well as CNS ischemia and infectious diseases, being
392 a potential neuroinflammation establishment mechanism (Kempuraj et al., 2016; Rochfort et
393 al., 2016). Stimulation of endothelial human brain cells (HCECs) with IL-6 was shown to
394 induce VEGF synthesis and release, promoting angiogenesis, alongside increased
395 expression of matrix metalloproteinase 9 (MMP9) (Yao et al., 2006). Increased MMPs

396 levels in different brain injury models were associated with degradation of the endothelial
397 basement membrane and enhanced tyrosine phosphorylation of tight junction proteins,
398 triggering protein redistribution, changes in adhesive properties between endothelial cells,
399 and TEER reduction, resulting in increased permeability (Stamatovic et al., 2008).

400 Although the roles of IL-6 have been pointed as essential to endothelial function,
401 angiogenesis and blood vessel stability have been classically described as depending on
402 anti-inflammatory TGF- β 1 cytokine signaling in the embryonic and adult brain (Dohgu et al.,
403 2004; Lebrin et al., 2005; Holderfield and Hughes, 2008; Arnold et al., 2014; Hellbach et al.,
404 2014; Siqueira et al., 2017). TGF- β 1 is a multifunctional cytokine that controls multiple
405 physiological and pathological events, such as embryogenesis, immune response, ECM
406 synthesis, cell differentiation and cell-cycle control in several tissues (Massague, 1998;
407 Massague and Gomis, 2006). TGF- β 1 in the CNS has been reported to play a key role in
408 neuronal generation, survival and migration (Brionne et al., 2003; Miller, 2003; Esposito et
409 al., 2005; Stipursky et al., 2012), glial differentiation (Sousa Vde et al., 2004; Romao et al.,
410 2008; Stipursky et al., 2014), and synapse formation (Diniz et al., 2012; Diniz et al., 2014).
411 More recently, our group demonstrated that TGF- β 1 secreted from RG cells induces
412 angiogenesis in the developing cerebral cortex (Siqueira et al., 2017). Herein, we observed
413 that CM from infected RG cells contains lower TGF- β 1 levels compared to uninfected cells.
414 Loss of the active form of TGF- β 1 cytokine, mutation of the *Tgfb1* gene or even deletion of
415 *Tgfr2* or *Alk5/Tgfr1* genes in endothelial cells of the embryonic forebrain have been shown
416 to promote excessive vascular sprouting, branching and induce cerebral hemorrhage
417 (Arnold et al., 2014). Furthermore, TGF- β 1 is known to promote tight junction proteins and
418 P-glycoprotein transporter expression in brain endothelial cells (Dohgu et al., 2004), induce
419 endothelial barrier properties, such as γ -glutamyl-transferase (GGT) expression, mediated
420 by astrocyte secretion (Garcia et al., 2004), and TGF- β signaling is involved in later stages
421 of blood vessel development, such as the induction of maturation and stability maintenance
422 mediating the interaction between endothelial and mural cells (Lebrin et al., 2005).

423 Here we demonstrated that Inf-RG-CM presented increased amounts of IL-6 and
424 significantly less TGF- β 1, compared to control RG-CM. Evidence shows that disruption of
425 endothelial interactions with neurovascular unit or low levels of TGF- β 1 leads to abnormal
426 distribution of junctional proteins and increased vascular permeability (Garcia et al., 2004;
427 Dohgu et al., 2005; Winkler et al., 2011), In the BBB, TGF- β 1 secretion by astrocytes has
428 been demonstrated as essential for maintaining brain vasculature stability and inhibiting or
429 decreasing leukocyte transmigration across the endothelium (Fabry et al., 1995; Alvarez et
430 al., 2013). Since mature BBB astrocytes are the main source of TGF- β 1, and RG cells also
431 secrete TGF- β 1, which we demonstrated as promoting RG-astrocyte differentiation
432 (Stipursky and Gomes, 2007; Stipursky et al., 2012, 2014), it is possible that, in our
433 infection model, reduced levels of RG-derived TGF- β 1, and possibly elevated levels of IL-6
434 proinflammatory cytokine, might impair endothelial ZO-1 tight junction organization and β -
435 catenin association in adherens junctions.

436 By adding TGF- β 1 to the Inf-RG-CM, there was a complete rescue of endothelial ZO-
437 1 protein levels, suggesting that *T. gondii* infection impairs TGF- β 1 expression/secretion, or
438 both, by RG cells.

439 In this context, alteration of RG secretome by *T. gondii* infection, may act as
440 underlying mechanisms of disruption of endothelial cell barrier properties. However, specific
441 downstream angiogenesis and vascular maturation molecular targets have not yet been
442 identified.

443 Herein, β -catenin has been pointed out as a potential target for RG-endothelial
444 dysfunctional interaction. The Wnt/ β -catenin pathway has been extensively investigated
445 and demonstrated as exerting critical roles on vascular development and maturation in the
446 developing cerebral cortex and maintenance of BBB in adult brain (Liebner et al., 2008;
447 Daneman et al., 2009; Ma et al., 2013; Engelhardt and Liebner, 2014). β -catenin, the
448 canonical downstream mediator of Wnt signaling, associates with classic cadherins in
449 adherens junctions and to α -catenin, that mediates its association with the actin

450 cytoskeleton. In endothelial cells, β -catenin is constitutively bound to VE-cadherin and when
451 β -catenin is free in cytoplasm, it is rapidly inactivated by phosphorylation and ubiquitination
452 by a protein complex that includes axin and adenomatous polyposis coli (APC). Upon
453 downregulation of VE-cadherin expression or Wnt signaling activation in endothelial cells,
454 β -catenin translocates to the nucleus to modulate gene expression, acting as a co-
455 transcription factor together with lymphoid enhancer factor/T-cell factor (Lef/TCF), Forkhead
456 box protein O1 (FoxO1), hypoxia-inducible factor (HIF), Smads and others, mediating
457 cellular responses such as cell cycle, apoptosis, cell differentiation and cell-cell
458 communication (Klaus and Birchmeier, 2008; Giannotta et al., 2013).

459 A previous report demonstrated that VE-cadherin phosphorylation prevents p120 and
460 β -catenin binding, triggering destabilization of adherens junctions, maintaining cells in a
461 mesenchymal state (Potter et al., 2005).

462 Endothelial cells adherens and tight junctions lay in close proximity to neighbor cells,
463 both mediating membrane adhesion and limiting paracellular permeability. Although
464 adherens and tight junctions are formed by distinct structural proteins, with specific binding
465 affinities, the assembly of tight junctions has been demonstrated as coupled with the
466 formation of adherens junctions. Physical linkages between these junctional structures can
467 be mediated by a multistep process that involves α -, β -catenins, ZO-1 and afadin proteins
468 interactions, initiating with adherens junctions protein clustering and structural organization
469 on cell membranes that later recruit and allow tight junctional machinery to assemble (for
470 revision Campbell et al., 2017). In fact, β -catenin/FoxO1 transcription factor complex was
471 demonstrated to repress Claudin-5 tight junction gene expression (Taddei et al., 2008). Ma
472 and colleagues (2013) demonstrated that Wnt/ β -catenin signaling activation can mediate
473 RG-endothelial interaction through transcriptionally induction of MMP2/MMP9 in endothelial
474 cells, which was correlated to decreased vessel stability and increased endothelial
475 proliferation in the developing cerebral cortex. Accordingly, increased MMPs levels were
476 found in astrocyte cultures (Lu and Lai, 2013) and in the sera of pregnant women infected
477 with *T. gondii* (Wang and Lai, 2013), suggesting that Wnt/ β -catenin signaling may modulate

478 junction protein levels expression and organization and/or turnover through multiple
479 mechanisms. Thus, in our context, *T. gondii* infection effects might exert critical function in
480 triggering endothelial junction dismantling, alongside β -catenin dissociation from cell-cell
481 contacts.

482 Together, our results suggest that *T. gondii* deregulates RG cells proliferation,
483 neurogenesis potential and secretory profile, with decreased TGF- β 1 and, to a less extent,
484 increase in IL-6 levels. In addition, the potential of RG cells to modulate endothelial cell
485 function is also affected by *T. gondii* infection, resulting in deficient organization of tight
486 junction protein ZO-1 and junction associated β -catenin, reduced TEER, leading to impaired
487 endothelial stabilization and loss of barrier properties. In a CT context, alterations in the
488 RG cell differentiation potential and in RG-endothelial cell interactions may be critical to the
489 reduced numbers of neurons generated during cortical development and dysfunctional BBB
490 formation, which would directly contribute to the establishment of the microcephaly
491 phenotype. Although RG-endothelial interactions are critical to promote vascular
492 development and BBB formation, the specific molecular mechanisms disrupted by *T. gondii*
493 infection in such interactions are not known. Thus, an improved description of the signaling
494 pathways involved in such events might contribute to the development of therapeutic
495 approaches to rescue or protect neural stem cells functions and vascular development, thus
496 preventing the clinical manifestations observed in CT.

497

498 **5) ACKNOWLEDGEMENTS**

499 We thank Dr. Flávia Carvalho Alcantara Gomes for providing equipment, laboratory
500 facility and some reagents; Marcelo Meloni, Adiel Batista do Nascimento and Sandra Maria
501 Oliveira Souza for technical assistance and Dr. José Morgado Diaz (INCA) and Dr. Luzia
502 Maria de Oliveira Pinto (IOC, Fiocruz) for the use of their MilliCell equipment.

503

504 **6) AUTHOR CONTRIBUTIONS STATEMENT**

505 DA performed bEnd.3 cultures, infection and TEER experiments. ACM performed
506 bEnd.3, treatments, immunocytochemistry quantifications and radial glia
507 immunocytochemistry quantifications. MS performed radial glia and bEnd.3
508 immunocytochemistry. CMC and MCW performed CBA and ELISA cytokines analysis,
509 respectively. JS performed radial glia cultures, bEnd.3 immunocytochemistry, TGF- β 1
510 ELISA and wrote the first draft of the manuscript. HSB discussed the experimental design
511 and data interpretation regarding *T. gondii* infection, provided equipment, laboratory facility
512 and some reagents. DA and JS equally contributed in the design of most of the
513 experiments. All authors contributed to manuscript revision, read and approved the
514 submitted version.

515

516 7) REFERENCES

- 517 Abbott, N.J. (2005). Dynamics of CNS barriers: evolution, differentiation, and
518 modulation. *Cell Mol Neurobiol* 25(1), 5-23.
- 519 Alvarez, J.I., Dodelet-Devillers, A., Kebir, H., Ifergan, I., Fabre, P.J., Terouz, S., et
520 al. (2011). The Hedgehog pathway promotes blood-brain barrier integrity and CNS
521 immune quiescence. *Science* 334(6063), 1727-1731. doi: 10.1126/science.1206936.
- 522 Alvarez, J.I., Katayama, T., and Prat, A. (2013). Glial influence on the blood brain
523 barrier. *Glia* 61(12), 1939-1958. doi: 10.1002/glia.22575.
- 524 Anderson, K.D., Pan, L., Yang, X.M., Hughes, V.C., Walls, J.R., Dominguez, M.G.,
525 et al. (2011). Angiogenic sprouting into neural tissue requires Gpr124, an orphan G
526 protein-coupled receptor. *Proc Natl Acad Sci U S A* 108(7), 2807-2812. doi:
527 10.1073/pnas.1019761108.
- 528 Arnold, T.D., Niaudet, C., Pang, M.F., Siegenthaler, J., Gaengel, K., Jung, B., et al.
529 (2014). Excessive vascular sprouting underlies cerebral hemorrhage in mice lacking
530 alphaVbeta8-TGFbeta signaling in the brain. *Development* 141(23), 4489-4499. doi:
531 10.1242/dev.107193.
- 532 Asano, T., Ito, H., Kariya, Y., Hoshi, K., Yoshihara, A., Ugawa, Y., et al. (2017).
533 Evaluation of blood-brain barrier function by quotient alpha2 macroglobulin and its
534 relationship with interleukin-6 and complement component 3 levels in
535 neuropsychiatric systemic lupus erythematosus. *PLoS One* 12(10), e0186414. doi:
536 10.1371/journal.pone.0186414.
- 537 Baeten, K.M., and Akassoglou, K. (2011). Extracellular matrix and matrix receptors
538 in blood-brain barrier formation and stroke. *Dev Neurobiol* 71(11), 1018-1039. doi:
539 10.1002/dneu.20954.
- 540 Barnabe-Heider, F., Wasylnka, J.A., Fernandes, K.J., Porsche, C., Sendtner, M.,
541 Kaplan, D.R., et al. (2005). Evidence that embryonic neurons regulate the onset of
542 cortical gliogenesis via cardiotrophin-1. *Neuron* 48(2), 253-265. doi:
543 10.1016/j.neuron.2005.08.037.
- 544 Bautch, V.L., and James, J.M. (2009). Neurovascular development: The beginning
545 of a beautiful friendship. *Cell Adh Migr* 3(2), 199-204.

- 546 Ben-Zvi, A., Lacoste, B., Kur, E., Andreone, B.J., Mayshar, Y., Yan, H., et al. (2014).
547 Mfsd2a is critical for the formation and function of the blood-brain barrier. *Nature*
548 509(7501), 507-511. doi: 10.1038/nature13324.
- 549 Briceño, M.P., Nascimento, L.A., Nogueira, N.P., Barenco, P.V., Ferro, E.A.,
550 Rezende-Oliveira, K., et al. (2016). Toxoplasma gondii Infection Promotes Epithelial
551 Barrier Dysfunction of Caco-2 Cells. *J Histochem Cytochem* 64(8), 459-469. doi:
552 10.1369/0022155416656349.
- 553 Brionne, T.C., Tesseur, I., Masliah, E., and Wyss-Coray, T. (2003). Loss of TGF-
554 beta 1 leads to increased neuronal cell death and microgliosis in mouse brain.
555 *Neuron* 40(6), 1133-1145.
- 556 Campbell, H.K., Maiers, J.L., and DeMali, K.A. (2017). Interplay between tight
557 junctions & adherens junctions. *Exp Cell Res* 358(1), 39-44. doi:
558 10.1016/j.yexcr.2017.03.061.
- 559 Carmeliet, P., and Jain, R.K. (2000). Angiogenesis in cancer and other diseases.
560 *Nature* 407(6801), 249-257. doi: 10.1038/35025220.
- 561 Daneman, R., Agalliu, D., Zhou, L., Kuhnert, F., Kuo, C.J., and Barres, B.A. (2009).
562 Wnt/beta-catenin signaling is required for CNS, but not non-CNS, angiogenesis. *Proc*
563 *Natl Acad Sci U S A* 106(2), 641-646. doi: 10.1073/pnas.0805165106.
- 564 Derada Troletti, C., de Goede, P., Kamermans, A., and de Vries, H.E. (2016).
565 Molecular alterations of the blood-brain barrier under inflammatory conditions: The
566 role of endothelial to mesenchymal transition. *Biochim Biophys Acta* 1862(3), 452-
567 460. doi: 10.1016/j.bbadis.2015.10.010.
- 568 Diniz, L.P., Almeida, J.C., Tortelli, V., Vargas Lopes, C., Setti-Perdigao, P.,
569 Stipursky, J., et al. (2012). Astrocyte-induced synaptogenesis is mediated by
570 transforming growth factor beta signaling through modulation of D-serine levels in
571 cerebral cortex neurons. *J Biol Chem* 287(49), 41432-41445. doi:
572 10.1074/jbc.M112.380824.
- 573 Diniz, L.P., Tortelli, V., Garcia, M.N., Araujo, A.P., Melo, H.M., Silva, G.S., et al.
574 (2014). Astrocyte transforming growth factor beta 1 promotes inhibitory synapse
575 formation via CaM kinase II signaling. *Glia* 62(12), 1917-1931. doi:
576 10.1002/glia.22713.
- 577 Dohgu, S., Takata, F., Yamauchi, A., Nakagawa, S., Egawa, T., Naito, M., et al.
578 (2005). Brain pericytes contribute to the induction and up-regulation of blood-brain
579 barrier functions through transforming growth factor-beta production. *Brain Res*
580 1038(2), 208-215. doi: 10.1016/j.brainres.2005.01.027.
- 581 Dohgu, S., Yamauchi, A., Takata, F., Naito, M., Tsuruo, T., Higuchi, S., et al. (2004).
582 Transforming growth factor-beta1 upregulates the tight junction and P-glycoprotein of
583 brain microvascular endothelial cells. *Cell Mol Neurobiol* 24(3), 491-497.
- 584 Engelhardt, B., and Liebner, S. (2014). Novel insights into the development and
585 maintenance of the blood-brain barrier. *Cell Tissue Res* 355(3), 687-699. doi:
586 10.1007/s00441-014-1811-2.
- 587 Errede, M., Girolamo, F., Rizzi, M., Bertossi, M., Roncali, L., and Virgintino, D.
588 (2014). The contribution of CXCL12-expressing radial glia cells to neuro-vascular
589 patterning during human cerebral cortex development. *Front Neurosci* 8, 324. doi:
590 10.3389/fnins.2014.00324.
- 591 Esposito, M.S., Piatti, V.C., Laplagne, D.A., Morgenstern, N.A., Ferrari, C.C.,
592 Pitossi, F.J., et al. (2005). Neuronal differentiation in the adult hippocampus
593 recapitulates embryonic development. *J Neurosci* 25(44), 10074-10086. doi:
594 10.1523/JNEUROSCI.3114-05.2005.
- 595 Fabry, Z., Topham, D.J., Fee, D., Herlein, J., Carlino, J.A., Hart, M.N., et al. (1995).
596 TGF-beta 2 decreases migration of lymphocytes in vitro and homing of cells into the
597 central nervous system in vivo. *J Immunol* 155(1), 325-332.
- 598 Ferguson, D.J., Bowker, C., Jeffery, K.J., Chamberlain, P., and Squier, W. (2013).
599 Congenital toxoplasmosis: continued parasite proliferation in the fetal brain despite
600 maternal immunological control in other tissues. *Clin Infect Dis* 56(2), 204-208. doi:
601 10.1093/cid/cis882.

- 602 Gan, X., Zhang, X., Cheng, Z., Chen, L., Ding, X., Du, J., et al. (2016). Toxoplasma
603 gondii inhibits differentiation of C17.2 neural stem cells through Wnt/beta-catenin
604 signaling pathway. *Biochem Biophys Res Commun* 473(1), 187-193. doi:
605 10.1016/j.bbrc.2016.03.076.
- 606 Garcia, C.M., Darland, D.C., Massingham, L.J., and D'Amore, P.A. (2004).
607 Endothelial cell-astrocyte interactions and TGF beta are required for induction of
608 blood-neural barrier properties. *Brain Res Dev Brain Res* 152(1), 25-38. doi:
609 10.1016/j.devbrainres.2004.05.008.
- 610 Giannotta, M., Trani, M., and Dejana, E. (2013). VE-cadherin and endothelial
611 adherens junctions: active guardians of vascular integrity. *Dev Cell* 26(5), 441-454.
612 doi: 10.1016/j.devcel.2013.08.020.
- 613 Gotz, M., and Barde, Y.A. (2005). Radial glial cells defined and major intermediates
614 between embryonic stem cells and CNS neurons. *Neuron* 46(3), 369-372. doi:
615 10.1016/j.neuron.2005.04.012.
- 616 Goumans, M.J., Lebrin, F., and Valdimarsdottir, G. (2003). Controlling the
617 angiogenic switch: a balance between two distinct TGF- β receptor signaling
618 pathways. *Trends Cardiovasc Med* 13(7), 301-307.
- 619 Hellbach, N., Weise, S.C., Vezzali, R., Wahane, S.D., Heidrich, S., Roidl, D., et al.
620 (2014). Neural deletion of Tgfb2 impairs angiogenesis through an altered secretome.
621 *Hum Mol Genet* 23(23), 6177-6190. doi: 10.1093/hmg/ddu338.
- 622 Hirota, S., Clements, T.P., Tang, L.K., Morales, J.E., Lee, H.S., Oh, S.P., et al.
623 (2015). Neuropilin 1 balances β 8 integrin-activated TGF β signaling to control
624 sprouting angiogenesis in the brain. *Development* 142(24), 4363-4373. doi:
625 10.1242/dev.113746.
- 626 Holderfield, M.T., and Hughes, C.C. (2008). Crosstalk between vascular endothelial
627 growth factor, notch, and transforming growth factor- β in vascular morphogenesis.
628 *Circ Res* 102(6), 637-652. doi: 10.1161/CIRCRESAHA.107.167171.
- 629 Kempuraj, D., Thangavel, R., Natteru, P.A., Selvakumar, G.P., Saeed, D., Zahoor,
630 H., Zaheer, S., Iyer, S.S. and Zaheer A. (2016). Neuroinflammation Induces
631 Neurodegeneration. *J Neurol Neurosurg Spine*. 1(1). pii: 1003.
- 632 Kessaris, N., Pringle, N., and Richardson, W.D. (2008). Specification of CNS glia
633 from neural stem cells in the embryonic neuroepithelium. *Philos Trans R Soc Lond B*
634 *Biol Sci* 363(1489), 71-85. doi: 10.1098/rstb.2006.2013.
- 635 Kim, J.H., Park, J.A., Lee, S.W., Kim, W.J., Yu, Y.S., and Kim, K.W. (2006). Blood-
636 neural barrier: intercellular communication at glio-vascular interface. *J Biochem Mol*
637 *Biol* 39(4), 339-345.
- 638 Klaus, A., and Birchmeier, W. (2009). Developmental signaling in myocardial
639 progenitor cells: a comprehensive view of Bmp- and Wnt/beta-catenin signaling.
640 *Pediatr Cardiol* 30(5), 609-616. doi: 10.1007/s00246-008-9352-7.
- 641 Konradt, C., Ueno, N., Christian, D.A., Delong, J.H., Pritchard, G.H., Herz, J., et al.
642 (2016). Endothelial cells are a replicative niche for entry of Toxoplasma gondii to the
643 central nervous system. *Nat Microbiol* 1, 16001. doi: 10.1038/nmicrobiol.2016.1.
- 644 Kriegstein, A., and Alvarez-Buylla, A. (2009). The glial nature of embryonic and adult
645 neural stem cells. *Annu Rev Neurosci* 32, 149-184. doi:
646 10.1146/annurev.neuro.051508.135600.
- 647 Lachenmaier, S.M., Deli, M.A., Meissner, M., and Liesenfeld, O. (2011). Intracellular
648 transport of Toxoplasma gondii through the blood-brain barrier. *J Neuroimmunol*
649 232(1-2), 119-130. doi: 10.1016/j.jneuroim.2010.10.029.
- 650 Lebrin, F., Deckers, M., Bertolino, P., and Ten Dijke, P. (2005). TGF- β receptor
651 function in the endothelium. *Cardiovasc Res* 65(3), 599-608. doi:
652 10.1016/j.cardiores.2004.10.036.
- 653 Liebner, S., Corada, M., Bangsow, T., Babbage, J., Taddei, A., Czupalla, C.J., et al.
654 (2008). Wnt/beta-catenin signaling controls development of the blood-brain barrier. *J*
655 *Cell Biol* 183(3), 409-417. doi: 10.1083/jcb.200806024.

- 656 Liebner, S., Czupalla, C.J., and Wolburg, H. (2011). Current concepts of blood-brain
657 barrier development. *Int J Dev Biol* 55(4-5), 467-476. doi: 10.1387/ijdb.103224sl.
- 658 Lu, C.Y., and Lai, S.C. (2013). Induction of matrix metalloproteinase-2 and -9 via
659 Erk1/2-NF-kappaB pathway in human astroglia infected with *Toxoplasma gondii*. *Acta*
660 *Trop* 127(1), 14-20. doi: 10.1016/j.actatropica.2013.03.004.
- 661 Ma, S., Kwon, H.J., Johng, H., Zang, K., and Huang, Z. (2013). Radial glial neural
662 progenitors regulate nascent brain vascular network stabilization via inhibition of Wnt
663 signaling. *PLoS Biol* 11(1), e1001469. doi: 10.1371/journal.pbio.1001469.
- 664 Massague, J. (1998). TGF-beta signal transduction. *Annu Rev Biochem* 67, 753-
665 791. doi: 10.1146/annurev.biochem.67.1.753.
- 666 Massague, J., and Gomis, R.R. (2006). The logic of TGFbeta signaling. *FEBS Lett*
667 580(12), 2811-2820. doi: 10.1016/j.febslet.2006.04.033.
- 668 Medici, D., Hay, E.D., and Goodenough, D.A. (2006). Cooperation between snail
669 and LEF-1 transcription factors is essential for TGF-beta1-induced epithelial-
670 mesenchymal transition. *Mol Biol Cell* 17(4), 1871-1879. doi: 10.1091/mbc.E05-08-
671 0767.
- 672 Miller, M.W. (2003). Expression of transforming growth factor-beta in developing rat
673 cerebral cortex: effects of prenatal exposure to ethanol. *J Comp Neurol* 460(3), 410-
674 424. doi: 10.1002/cne.10658.
- 675 Montoya, J.G., and Liesenfeld, O. (2004). Toxoplasmosis. *Lancet* 363(9425), 1965-
676 1976. doi: 10.1016/S0140-6736(04)16412-X.
- 677 Mostert, D.K., and Silver, J. (2003). Precursors of neurons, neuroglia, and
678 ependymal cells in the CNS: what are they? Where are they from? How do they get
679 where they are going? *Glia* 43(1), 6-18. doi: 10.1002/glia.10238.
- 680 Nakamura, M., Okada, S., Toyama, Y., and Okano, H. (2005). Role of IL-6 in spinal
681 cord injury in a mouse model. *Clin Rev Allergy Immunol* 28(3), 197-204. doi:
682 10.1385/CRIAL:28:3:197.
- 683 Neu, N., Duchon, J., and Zachariah, P. (2015). TORCH infections. *Clin Perinatol*
684 42(1), 77-103, viii. doi: 10.1016/j.clp.2014.11.001.
- 685 Noctor, S.C., Flint, A.C., Weissman, T.A., Dammerman, R.S., and Kriegstein, A.R.
686 (2001). Neurons derived from radial glial cells establish radial units in neocortex.
687 *Nature* 409(6821), 714-720. doi: 10.1038/35055553.
- 688 Nogueira, A.R., Leve, F., Morgado-Diaz, J., Tedesco, R.C., and Pereira, M.C.
689 (2016). Effect of *Toxoplasma gondii* infection on the junctional complex of retinal
690 pigment epithelial cells. *Parasitology* 143(5), 568-575. doi:
691 10.1017/S0031182015001973.
- 692 Ortega, J.A., and Alcantara, S. (2010). BDNF/MAPK/ERK-induced BMP7
693 expression in the developing cerebral cortex induces premature radial glia
694 differentiation and impairs neuronal migration. *Cereb Cortex* 20(9), 2132-2144. doi:
695 10.1093/cercor/bhp275.
- 696 Pepper, M.S. (1997). Transforming growth factor-beta: vasculogenesis,
697 angiogenesis, and vessel wall integrity. *Cytokine Growth Factor Rev* 8(1), 21-43.
- 698 Potter, M.D., Barbero, S., and Cheresh, D.A. (2005). Tyrosine phosphorylation of
699 VE-cadherin prevents binding of p120- and beta-catenin and maintains the cellular
700 mesenchymal state. *J Biol Chem* 280(36), 31906-31912. doi:
701 10.1074/jbc.M505568200.
- 702 Rakic, P. (1971). Neuron-glia relationship during granule cell migration in developing
703 cerebellar cortex. A Golgi and electronmicroscopic study in *Macacus Rhesus*. *J Comp*
704 *Neurol* 141(3), 283-312. doi: 10.1002/cne.901410303.
- 705 Rakic, P. (1999). Neurobiology. Discriminating migrations. *Nature* 400(6742), 315-
706 316. doi: 10.1038/22427.
- 707 Rochfort, K.D., Collins, L.E., McLoughlin, A., and Cummins, P.M. (2016). Tumour
708 necrosis factor-alpha-mediated disruption of cerebrovascular endothelial barrier
709 integrity in vitro involves the production of proinflammatory interleukin-6. *J*
710 *Neurochem* 136(3), 564-572. doi: 10.1111/jnc.13408.

- 711 Romao, L.F., Sousa Vde, O., Neto, V.M., and Gomes, F.C. (2008). Glutamate
712 activates GFAP gene promoter from cultured astrocytes through TGF-beta1
713 pathways. *J Neurochem* 106(2), 746-756. doi: 10.1111/j.1471-4159.2008.05428.x.
- 714 Schiavone, S., Mhillaj, E., Neri, M., Morgese, M.G., Tucci, P., Bove, M., et al.
715 (2017). Early Loss of Blood-Brain Barrier Integrity Precedes NOX2 Elevation in the
716 Prefrontal Cortex of an Animal Model of Psychosis. *Mol Neurobiol* 54(3), 2031-2044.
717 doi: 10.1007/s12035-016-9791-8.
- 718 Siqueira, M., Francis, D., Gisbert, D., Gomes, F.C.A., and Stipursky, J. (2017).
719 Radial Glia Cells Control Angiogenesis in the Developing Cerebral Cortex Through
720 TGF-beta1 Signaling. *Mol Neurobiol*. doi: 10.1007/s12035-017-0557-8.
- 721 Song, H.B., Jun, H.O., Kim, J.H., Lee, Y.H., Choi, M.H., and Kim, J.H. (2017).
722 Disruption of outer blood-retinal barrier by Toxoplasma gondii-infected monocytes is
723 mediated by paracrinely activated FAK signaling. *PLoS One* 12(4), e0175159. doi:
724 10.1371/journal.pone.0175159.
- 725 Sousa Vde, O., Romao, L., Neto, V.M., and Gomes, F.C. (2004). Glial fibrillary
726 acidic protein gene promoter is differently modulated by transforming growth factor-
727 beta 1 in astrocytes from distinct brain regions. *Eur J Neurosci* 19(7), 1721-1730. doi:
728 10.1111/j.1460-9568.2004.03249.x.
- 729 Souza, B.S., Sampaio, G.L., Pereira, C.S., Campos, G.S., Sardi, S.I., Freitas, L.A.,
730 et al. (2016). Zika virus infection induces mitosis abnormalities and apoptotic cell
731 death of human neural progenitor cells. *Sci Rep* 6, 39775. doi: 10.1038/srep39775.
- 732 Stamatovic, S.M., Keep, R.F., and Andjelkovic, A.V. (2008). Brain endothelial cell-
733 cell junctions: how to "open" the blood brain barrier. *Curr Neuropharmacol* 6(3), 179-
734 192. doi: 10.2174/157015908785777210.
- 735 Stipursky, J., Francis, D., Dezone, R.S., Bergamo de Araujo, A.P., Souza, L.,
736 Moraes, C.A., et al. (2014). TGF-beta1 promotes cerebral cortex radial glia-astrocyte
737 differentiation in vivo. *Front Cell Neurosci* 8, 393. doi: 10.3389/fncel.2014.00393.
- 738 Stipursky, J., Francis, D., and Gomes, F.C. (2012). Activation of MAPK/PI3K/SMAD
739 pathways by TGF-beta(1) controls differentiation of radial glia into astrocytes in vitro.
740 *Dev Neurosci* 34(1), 68-81. doi: 10.1159/000338108.
- 741 Stipursky, J., and Gomes, F.C. (2007). TGF-beta1/SMAD signaling induces
742 astrocyte fate commitment in vitro: implications for radial glia development. *Glia*
743 55(10), 1023-1033. doi: 10.1002/glia.20522.
- 744 Taddei, A., Giampietro, C., Conti, A., Orsenigo, F., Breviario, F., Pirazzoli, V., et al.
745 (2008). Endothelial adherens junctions control tight junctions by VE-cadherin-
746 mediated upregulation of claudin-5. *Nat Cell Biol* 10(8), 923-934. doi:
747 10.1038/ncb1752.
- 748 Taga, T., and Fukuda, S. (2005). Role of IL-6 in the neural stem cell differentiation.
749 *Clin Rev Allergy Immunol* 28(3), 249-256. doi: 10.1385/CRIAI:28:3:249.
- 750 Takahashi, T., Takase, Y., Yoshino, T., Saito, D., Tadokoro, R., and Takahashi, Y.
751 (2015). Angiogenesis in the developing spinal cord: blood vessel exclusion from
752 neural progenitor region is mediated by VEGF and its antagonists. *PLoS One* 10(1),
753 e0116119. doi: 10.1371/journal.pone.0116119.
- 754 Uchida, T., Mori, M., Uzawa, A., Masuda, H., Muto, M., Ohtani, R., et al. (2017).
755 Increased cerebrospinal fluid metalloproteinase-2 and interleukin-6 are associated
756 with albumin quotient in neuromyelitis optica: Their possible role on blood-brain
757 barrier disruption. *Mult Scler* 23(8), 1072-1084. doi: 10.1177/1352458516672015.
- 758 Wallon, M., Liou, C., Garner, P., and Peyron, F. (1999). Congenital toxoplasmosis:
759 systematic review of evidence of efficacy of treatment in pregnancy. *BMJ* 318(7197),
760 1511-1514.
- 761 Wang, M.F., and Lai, S.C. (2013). Fibronectin degradation by MMP-2/MMP-9 in the
762 serum of pregnant women and umbilical cord with Toxoplasma gondii infection. *J*
763 *Obstet Gynaecol* 33(4), 370-374. doi: 10.3109/01443615.2013.769501.
- 764 Wang, T., Zhou, J., Gan, X., Wang, H., Ding, X., Chen, L., et al. (2014). Toxoplasma
765 gondii induce apoptosis of neural stem cells via endoplasmic reticulum stress
766 pathway. *Parasitology* 141(7), 988-995. doi: 10.1017/S0031182014000183.

767 Winkler, E.A., Bell, R.D., and Zlokovic, B.V. (2011). Central nervous system
768 pericytes in health and disease. *Nat Neurosci* 14(11), 1398-1405. doi:
769 10.1038/nn.2946.

770 Wylezinski, L.S., and Hawiger, J. (2016). Interleukin 2 Activates Brain Microvascular
771 Endothelial Cells Resulting in Destabilization of Adherens Junctions. *J Biol Chem*
772 291(44), 22913-22923. doi: 10.1074/jbc.M116.729038.

773 Xiao, J., Kannan, G., Jones-Brando, L., Brannock, C., Krasnova, I.N., Cadet, J.L., et
774 al. (2012). Sex-specific changes in gene expression and behavior induced by chronic
775 *Toxoplasma* infection in mice. *Neuroscience* 206, 39-48. doi:
776 10.1016/j.neuroscience.2011.12.051.

777 Yao, J.S., Zhai, W., Young, W.L., and Yang, G.Y. (2006). Interleukin-6 triggers
778 human cerebral endothelial cells proliferation and migration: the role for KDR and
779 MMP-9. *Biochem Biophys Res Commun* 342(4), 1396-1404. doi:
780 10.1016/j.bbrc.2006.02.100.

781 Zhang, X., Su, R., Cheng, Z., Zhu, W., Li, Y., Wang, Y., et al. (2017). A mechanistic
782 study of *Toxoplasma gondii* ROP18 inhibiting differentiation of C17.2 neural stem
783 cells. *Parasit Vectors* 10(1), 585. doi: 10.1186/s13071-017-2529-2.

784 Zhao, Z., Nelson, A.R., Betsholtz, C., and Zlokovic, B.V. (2015). Establishment and
785 Dysfunction of the Blood-Brain Barrier. *Cell* 163(5), 1064-1078. doi:
786 10.1016/j.cell.2015.10.067.

787

788 FIGURES LEGENDS

789

790 **Figure 1. *T. gondii* infection decreases Radial glia cell proliferation and**
791 **neurogenic potential.**

792 Infection of RG cells cultures with *T. gondii* tachyzoites for 24 h significantly
793 decreased the number of Nestin/BLBP double labeled cells number, compared with control
794 (A-C) which was accompanied by reduced numbers of proliferative Ki67/Nestin positive
795 cells compared with control uninfected cells (D-F). A significant decrease in generation of
796 β -III-tubulin positive neuron numbers was induced by *T. gondii* infection, when compared
797 with control (G-I). RG differentiation into GFAP positive astrocytes was not affected by *T.*
798 *gondii* infection when compared to controls (J-L). *T. gondii* infection induced significant
799 changes in the percentage of cell composition in RG cultures compared to controls (M).
800 *P=0.0423, **P=0.0019, ***P=0.0001 versus controls, unpaired *t* test.

801

802 **Figure 2. Conditioned medium from *T. gondii*-infected Radial glia decreases ZO-**
803 **1/ β -catenin proteins organization and impairs barrier properties of brain**

804 **microvascular endothelial cells.** Murine brain endothelial cells (bEnd.3) were incubated
805 for 24h with cultivation medium (Control), conditioned medium derived from uninfected RG
806 cultures (RG-CM) or conditioned medium derived from *T. gondii*-infected RG cultures (Inf-
807 RG-CM). ZO-1 tight junction adapter protein was found mainly distributed along adjacent
808 cell membranes of confluent control cultures (A). Addition of RG-CM to endothelial
809 monolayers significantly increased the levels of ZO-1 proteins on cells surfaces (B, E).
810 bEnd.3 cells incubated with Inf-RG-CM (C, E) presented reduced levels of ZO-1
811 immunoreactivity, when compared with controls (A-E). Tight junction organization index in
812 cell-cell contact regions (TiJOR) was also increased by addition RG-CM, when compared
813 with control cultures, and significantly disrupted by Inf-RG-CM presenting as discontinuous
814 ZO-1 labeling, when compared with RG-CM-treated cultures (F). Transendothelial electrical
815 resistance (TEER) was significantly increased by RG-CM when compared to all conditions.
816 Inf-RG-CM treatment impaired RG potential to induce TEER by reducing electrical
817 resistance on bEnd.3 cells below control levels (G). In Control cultures β -catenin was found
818 associated with cell-cell junctional contacts, similar to ZO-1 tight junction distribution (H, K,
819 N). Addition of RG-CM to endothelial monolayers enhanced β -catenin immunoreactivity and
820 similar to ZO-1 protein on cells contacts regions (I, L, O). bEnd.3 cells incubated with Inf-
821 RG-CM presented reduced immunoreactivity for β -catenin similar to ZO-1, concomitant with
822 junctions disorganization (J, M, P) when compared with controls (A-C). β -catenin
823 distribution in infected cells were mainly displaced to intracellular parasites *P=0.03,
824 **P=0.0001, one-way ANOVA with Bonferroni post-test.

825

826

827 **Figure 3. *T. gondii* infection alters the levels of secreted cytokines by Radial**
828 **glia cells.** Conditioned medium from uninfected RG cultures (RG-CM) and from cultures
829 infected with *T. gondii* tachyzoites for 24 h (Inf-RG-CM), were subjected to Cytokine Bead
830 Array (CBA) and ELISA assays to measure the levels of pro and anti-inflammatory secreted
831 cytokines. CBA detected augmented levels of IL-6 and ELISA revealed decreased TGF- β 1

832 levels (A) in Inf-RG-CM, compared with RG-CM. Addition of TGF- β 1 (19=0ng/mL) to Inf-
833 RG-CM significantly rescued the levels of ZO-1 labeling intensity, similar to addition of TGF-
834 β 1 alone to bEnd.3 cells, when compared to RG-CM. **p=0.0001, *p=0.036, one-way
835 ANOVA with Bonferroni post-test.

836 .

837 **Supplementary figure 1. Identification of *T. gondii* tachyzoites in infected cells.**

838 RG cultures were infected with *T. gondii* tachyzoites for 24h and labelled with DAPI to
839 identify host cell nucleus and parasite DNA (blue). Uninfected RG cultures labeled with
840 DAPI and Nestin (red) (A, B). Infected RG cells showing host and tachyzoites DNA in the
841 cytoplasm (C, D, arrows), high magnification of tachyzoites in infected cells (D', D'').

842

843 **Supplementary figure 2. *T. gondii* infection does not affect RG and neuronal cell**

844 **death.** RG cultures were infected with *T. gondii* tachyzoites for 2h and and labelled with
845 neuronal marker (β Tubulin), RG marker (Nestin) and apoptotic cell marker (cleaved-
846 Caspase 3), No statistic differences in the percentage of β -tubulinIII/Caspase3 (A, C) and
847 Nestin/Caspase3 (B, D) double positive cells were observed. Quantification of total DAPI-
848 labeled nucleus per microscopical field in uninfected and infected RG cultures revealed no
849 significant difference in total cells number in both conditions (E). P>0.05, unpaired *t*-test.

850

851

852

853

854

855

856

857

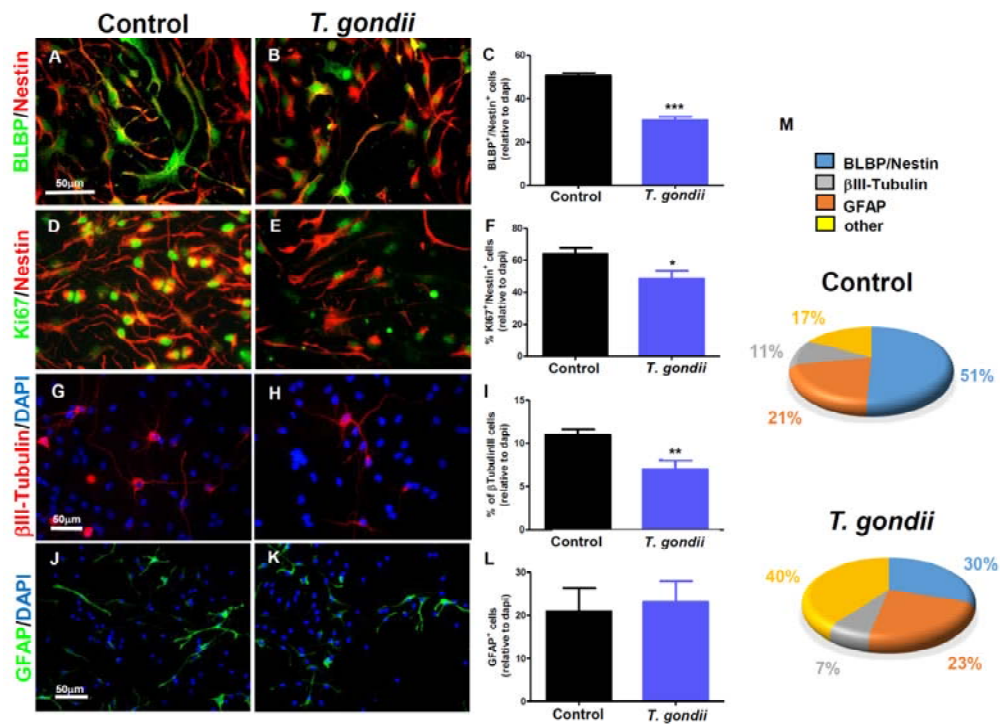
858

859

860

861
862
863
864
865
866
867
868
869

Figure 1.



870
871
872
873
874
875

876

877

878

879

880

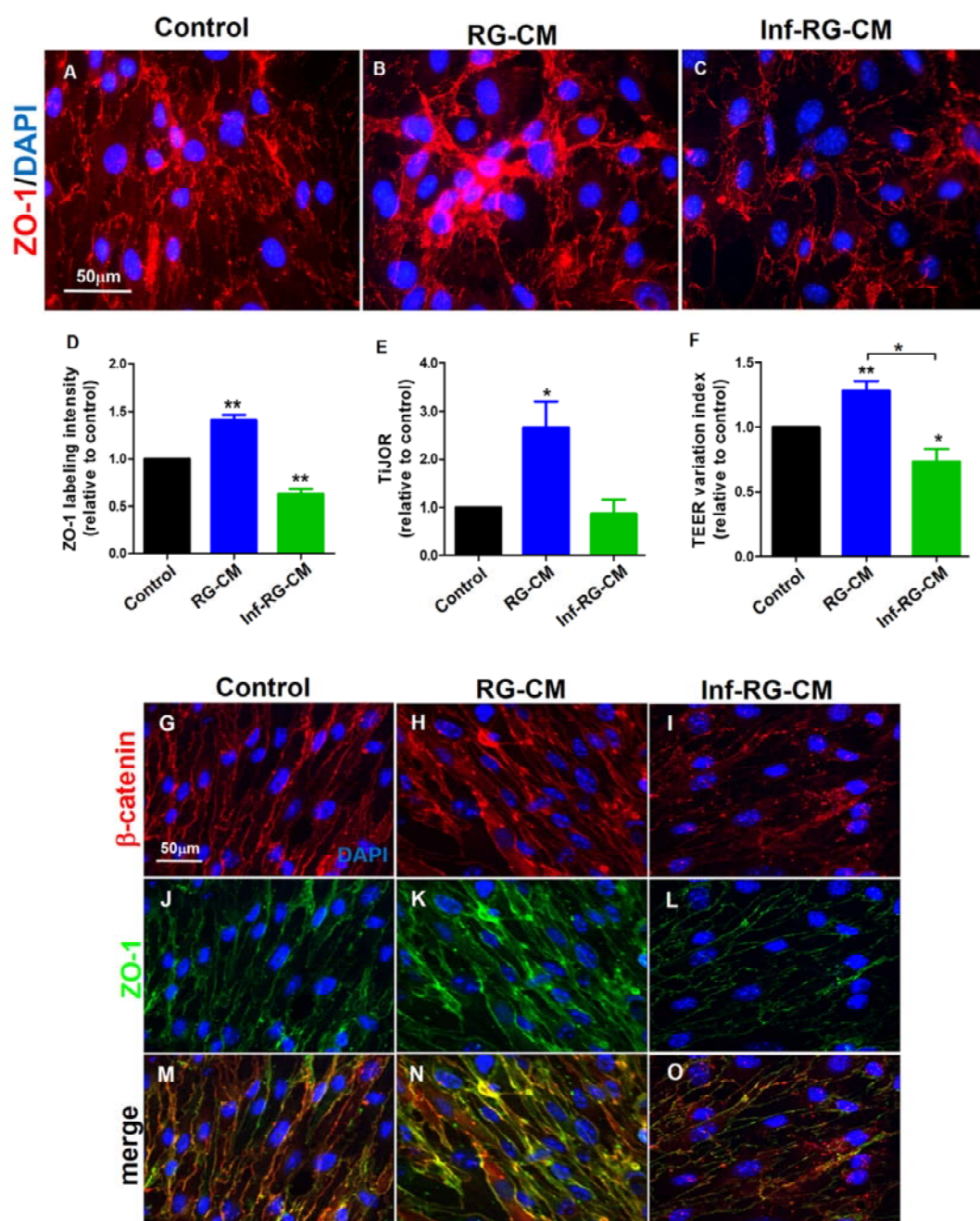
881

882

883

884

Figure 2.



885

886

887

888

889

890

891

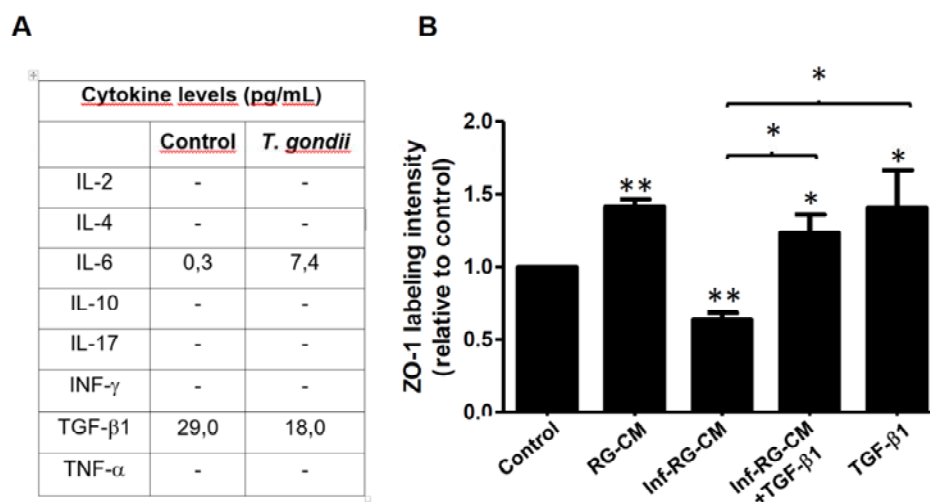
892

893

894

895

Figure 3.



896

897

898

899

900

901

902

903

904

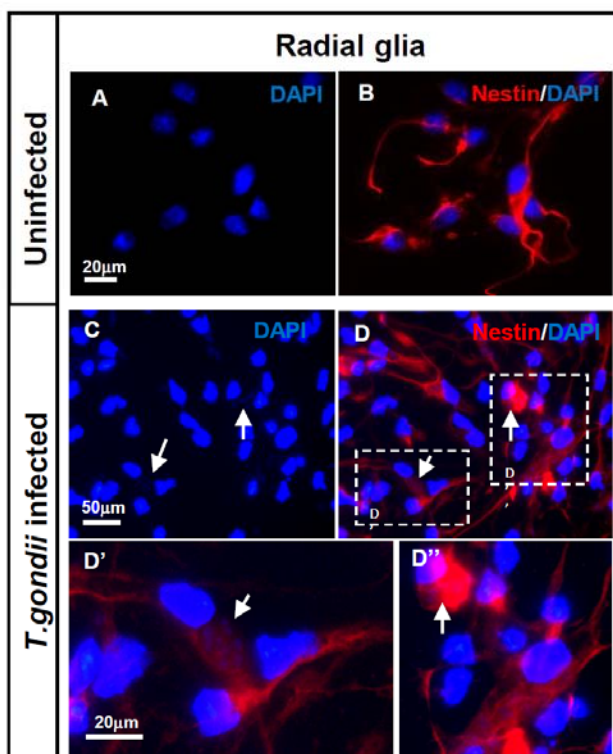
905

906

907

908

Supplementary Figure 1.



909

910

911

912

913

914

915

916

917

918

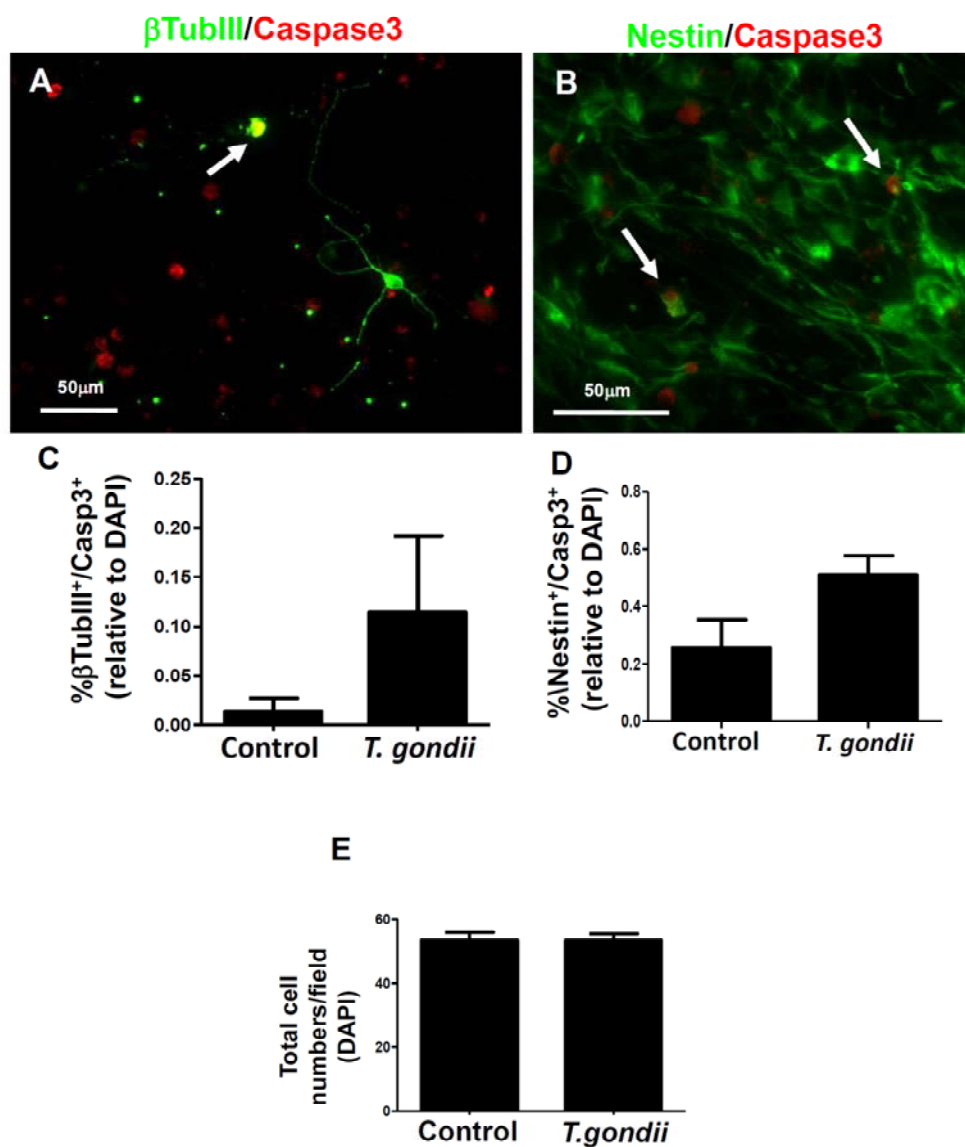
919

920

921

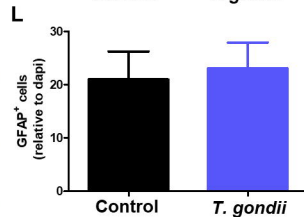
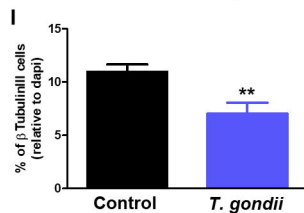
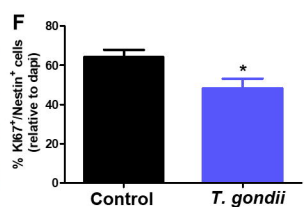
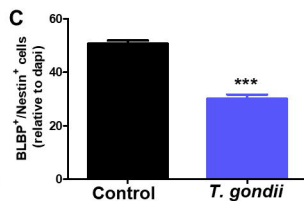
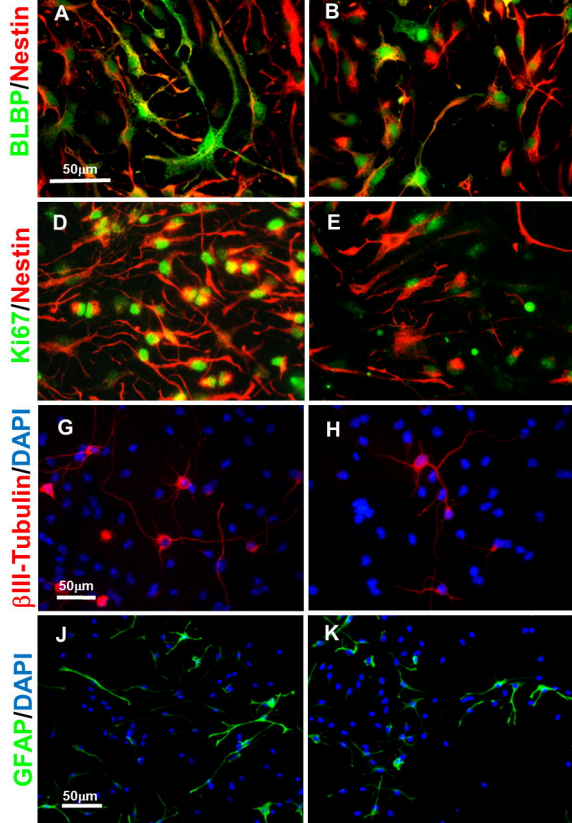
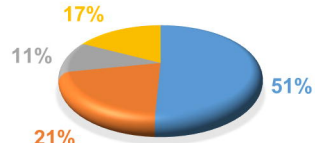
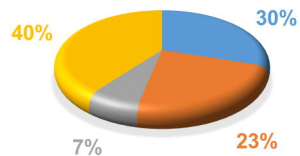
922

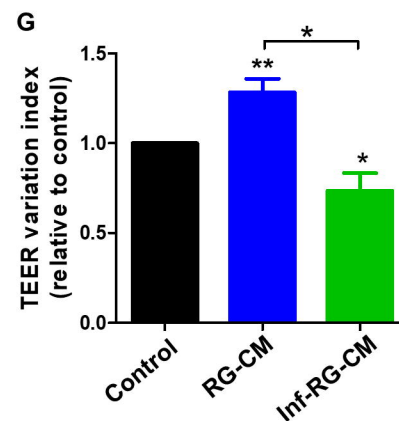
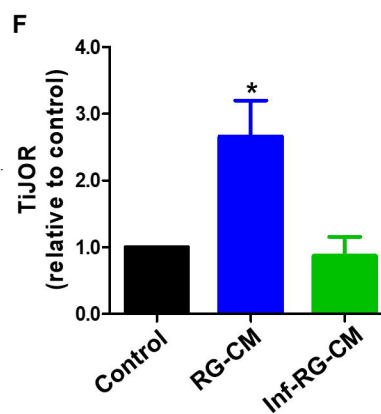
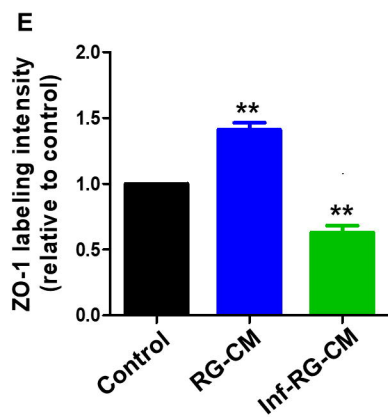
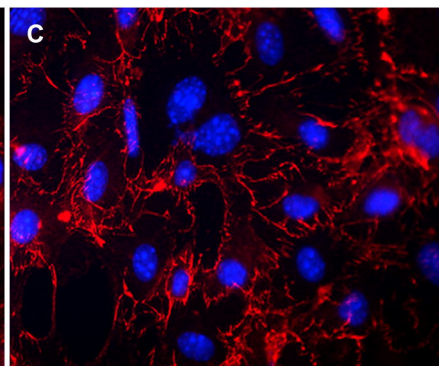
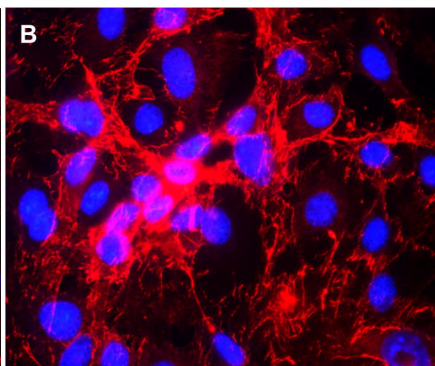
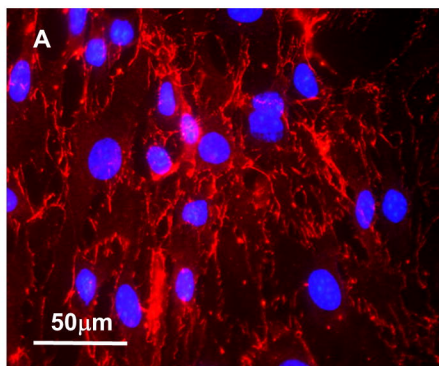
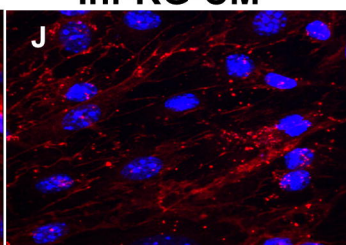
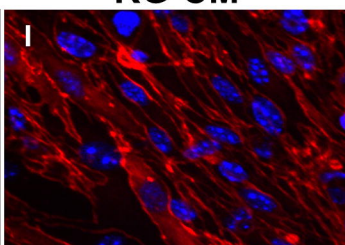
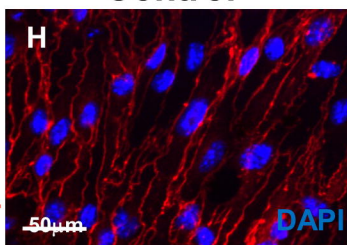
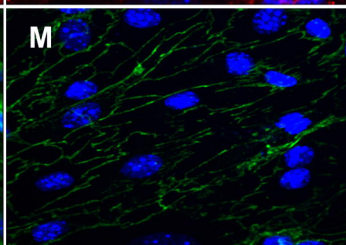
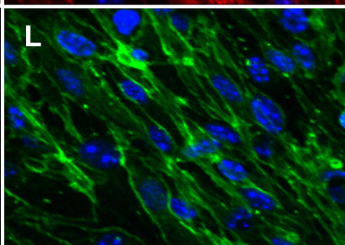
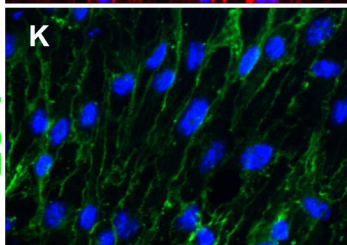
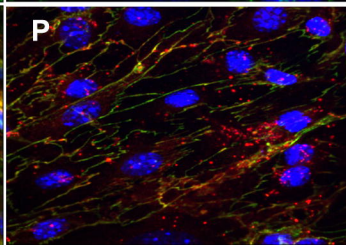
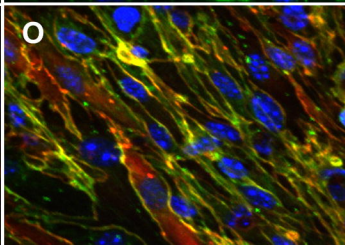
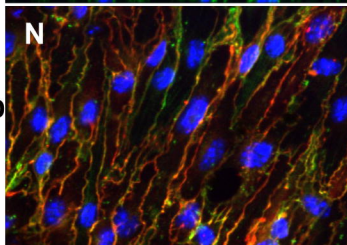
Supplementary Figure 2.



923

924

Control***T. gondii*****M****Control*****T. gondii***

Control**RG-CM****Inf-RG-CM****ZO-1/DAPI****Control****RG-CM****Inf-RG-CM** **β -catenin****ZO-1****merge**

A

<u>Cytokine levels (pg/mL)</u>		
	<u>Control</u>	<u><i>T. gondii</i></u>
IL-2	-	-
IL-4	-	-
IL-6	0,3	7,4
IL-10	-	-
IL-17	-	-
INF- γ	-	-
TGF- β 1	29,0	18,0
TNF- α	-	-

B